applied sciences

IMPACT FACTOR 2.7

CITESCORE 4.5

Article

A Microscopic Traffic Model Considering Time Headway and Distance Headway

Faryal Ali, Zawar Hussain Khan, Ahmed B. Altamimi, Khurram Shehzad Khattak and Thomas Aaron Gulliver

MDPI

https://doi.org/10.3390/app13127234

applied sciences

MDPI

Article

A Microscopic Traffic Model Considering Time Headway and Distance Headway

Faryal Ali [1,*], Zawar Hussain Khan [1], Ahmed B. Altamimi [2], Khurram Shehzad Khattak [3] and Thomas Aaron Gulliver [1]

[1] Department of Electrical and Computer Engineering, University of Victoria, Victoria, BC V8W 2Y2, Canada; khanz@uvic.ca (Z.H.K.); agullive@ece.uvic.ca (T.A.G.)
[2] College of Computer Science and Software Engineering, University of Hail, Hail 55476, Saudi Arabia; altamimi.a@uoh.edu.sa
[3] Department of Computer System Engineering, University of Engineering and Technology, Peshawar 25000, Pakistan; khurram.s.khattak@gmail.com
* Correspondence: faryalali@uvic.ca

Featured Application: Authors are encouraged to provide a concise description of the specific application or a potential application of the work. This section is not mandatory.

Abstract: A microscopic traffic model is presented which employs differences in velocity to characterize driver behavior. The Intelligent Driver (ID) model is based on an acceleration constant which cannot capture different traffic conditions. Further, it is not based on traffic physics and so can produce inaccurate results. The proposed model is an improved ID model and both are evaluated on a 2000 m circular road. The results obtained show that the proposed model can appropriately characterize traffic flow and density. Further, the variations in flow and velocity are smoother than with the ID model. This is because the proposed model is based on actual traffic parameters rather than an unrealistic traffic exponent.

Keywords: velocity difference; microscopic traffic flow; acceleration constant; Intelligent Driver (ID) model

check for updates

Citation: Ali, F.; Khan, Z.H.; Altamimi, A.B.; Khattak, K.S.; Gulliver, T.A. A Microscopic Traffic Model Considering Time Headway and Distance Headway. *Appl. Sci.* **2023**, *13*, 7234. https://doi.org/10.3390/app13127234

Academic Editor: Alessandro Lo Schiavo

Received: 3 May 2023
Revised: 5 June 2023
Accepted: 8 June 2023
Published: 17 June 2023

Copyright: © 2023 by the authors. Licensee MDPI, Basel, Switzerland. This article is an open access article distributed under the terms and conditions of the Creative Commons Attribution (CC BY) license (https://creativecommons.org/licenses/by/4.0/).

1. Introduction

Traffic modeling plays a vital role in the planning, management, and development of road networks [1]. This requires accurate and realistic characterization of traffic behavior [2,3]. Traffic models have been extensively used to mitigate congestion [4] because it is a key concern in urban areas around the globe. Congestion causes excessive fuel consumption, air pollution, and safety issues, and has an adverse economic impact [4–6].

It has been shown that nearly 88 billion dollars were lost due to congestion in the United States in 2019 [7]. The increasing number of vehicles on the roads adds to congestion. For example, there were 284.5 million cars registered in the United States in 2019, and this increased by 0.84% in 2020 [8]. Large traffic queues are created during congestion which impede the smooth flow of traffic. Traffic flow is influenced by the time and space required for vehicles to adjust to the environment [9]. These factors affect driver response and result in velocity differences.

Three types of models are commonly used to characterize traffic: macroscopic, microscopic, and mesoscopic. Macroscopic models consider collective vehicle behavior and are typically used to determine velocity, flow, and density [10]. Microscopic models consider individual vehicle behavior using parameters such as time and distance headways, position, and velocity [11]. They are used to predict vehicle dynamics and are often based on driver response [12]. Mesoscopic models are a hybrid of microscopic and macroscopic models and so share the properties of both [13].

Pipes [14] and Reuschel [15] were the first to introduce microscopic traffic models. Velocity was determined using the distance between following and leading vehicles. However, their models are simplistic and cannot adequately characterize traffic behavior [16]. Newell [17] introduced a model which considers distance headway and velocity. With this model, large distance headways can produce high velocities and low-density traffic [5]. However, it can also create excessive acceleration, which is unrealistic. In [18], an Optimal Velocity Model (OVM) was proposed which depicts a constant driver response regardless of the traffic conditions. This is not a realistic characterization as traffic and velocity differences are ignored, leading to unstable dynamics [9]. Moreover, the acceleration can be very high when the velocity is far from the equilibrium distribution, and the density is not considered. It has been shown that this model leads to traffic accidents because of the small distances between vehicles.

Helbing and Tilch [19] introduced the Generalized Force Model (GFM) which employs negative velocity differences considering following vehicles and the OVM. Unfortunately, it can produce unrealistic results as there are rapid changes in acceleration. This is because only aggressive drivers are considered so slow and typical driver behavior is ignored [9]. This model was improved in [20] using both negative and positive velocity differences [5]. Gipps [21] developed a different traffic model but the acceleration is not realistic [16]. In addition, the behavior may not correspond to the model parameters [22].

Treiber et al. [22] developed the Intelligent Driver (ID) model which is an improvement of the Gipps model [21]. Driver behavior is considered along with distance headway and velocity to provide smooth acceleration [23,24]. The ID model has been used to avoid collisions during emergencies [25], and the results are similar to those obtained when observing real traffic [26]. However, it employs an acceleration constant δ which is the same for all traffic conditions, so traffic physics is ignored. The ID model was modified in [27] for traffic at signalized intersections. However, a value of $\delta = 4$ was employed, so real traffic conditions were neglected [28]. This constant was chosen as the best fit for general traffic environments. A similar approach was employed in [29] for deceleration at intersections. In this case, the distances between vehicles are very small even with a high velocity, which is unrealistic [9]. The ID model has been incorporated in MovSim to evaluate longitudinal vehicle movement [25] and also in PTV VISSIM and Simulation of Urban Mobility (SUMO). However, driver behavior is not considered in this model [30].

One application of the ID model is with Connected and Autonomous Vehicles (CAVs) to improve traffic safety and passenger comfort [31,32]. Li et al. [33] employed this model to characterize the car-following behavior of CAVs, while Schakel et al. [34] proposed an improved ID model to explore CAV traffic stability. In this case, there is an abrupt decrease in velocity when the density reaches half its maximum (critical density), which is unrealistic as the velocity should be smooth. A modified ID model was proposed in [35] to better characterize real traffic conditions. However, CAV behavior with this model is not realistic because under actual traffic conditions, the drivers take longer to achieve a smooth car-following behavior and the variations in headway are greater [36]. The ID model has also been incorporated into cooperative and Adaptive Cruise Control (ACC) systems [37,38]. Unfortunately, the safe distance between vehicles with this model is too small when the velocity is high, which can result in accidents when employed in ACC and related systems.

A model is introduced here to realistically characterize traffic flow based on velocity differences and driver sensitivity. This improves the ID model which can produce unrealistic traffic behavior because of the constant acceleration exponent. Driver response to changes in velocity is known as sensitivity. The interval for a vehicle to adapt to variations in traffic conditions is referred to as the distance headway, while the time required to traverse this interval is known as the time headway. Both the proposed and ID models are evaluated for a platoon of 52 vehicles on a circular road of length 2000 m with periodic boundary conditions. The results obtained demonstrate that the proposed model provides better traffic characterization than the ID model.

2. Traffic Models

The ID model is a car-following model based on the behavior of leading vehicles. The acceleration is determined by the velocity, distance headway, and driver response which is $\frac{v}{v_d}$, where v and v_d are the average and the desired velocities, respectively. The acceleration is [22]

$$\dot{v} = a_m \left(1 - \left(\frac{v}{v_d}\right)^{\delta} - \left(\frac{s^*}{h}\right)^2\right), \tag{1}$$

where a_m is the maximum acceleration, δ is the acceleration constant, and h is the distance headway as illustrated in Figure 1. The desired distance headway is [22]

$$s^* = J + \tau v + \frac{v\Delta v}{2\sqrt{a_m b}} \tag{2}$$

where J is the jam spacing during congestion, τ is the time headway, Δv is the change in velocity, and b is the minimum acceleration.

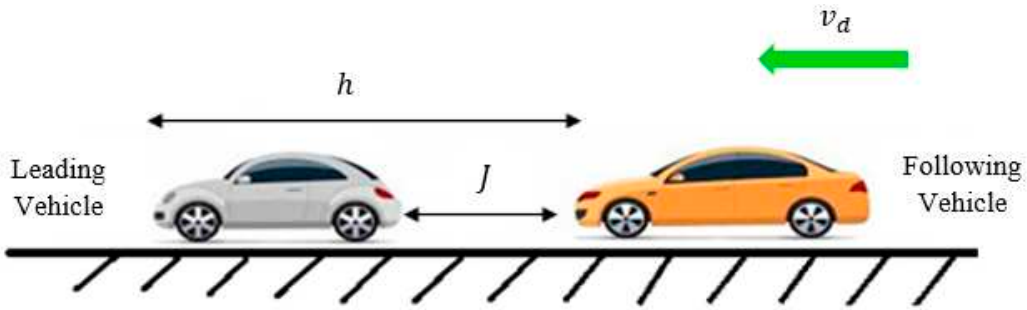

Figure 1. Traffic model parameters.

With the ID model, traffic behavior is determined by the exponent δ. However, this fixed value is inadequate for diverse traffic scenarios. Further, it is not based on real vehicle dynamics so poor results can occur. Hence, a variable exponent is proposed which is based on the difference in velocity between forward and rearward vehicles. This difference is given by

$$V = v_f - v_r \tag{3}$$

where v_f is the forward vehicle velocity and v_r is the rearward vehicle velocity as shown in Figure 2. The product of velocity and density is the traffic flow [23]

$$F = \rho v \tag{4}$$

and substituting Equation (4) in Equation (3) gives

$$V = \left(\frac{F}{\rho}\right)_f - \left(\frac{F}{\rho}\right)_r \tag{5}$$

A high density results in slow vehicles and a small distance headway h. Conversely, a low density results in a large distance headway between vehicles and large vehicle speeds [9]. Further, the time headway τ is inversely proportional to the flow [39], so Equation (5) can be expressed as

$$V = \frac{h_f}{\tau_f} - \frac{h_r}{\tau_r} \tag{6}$$

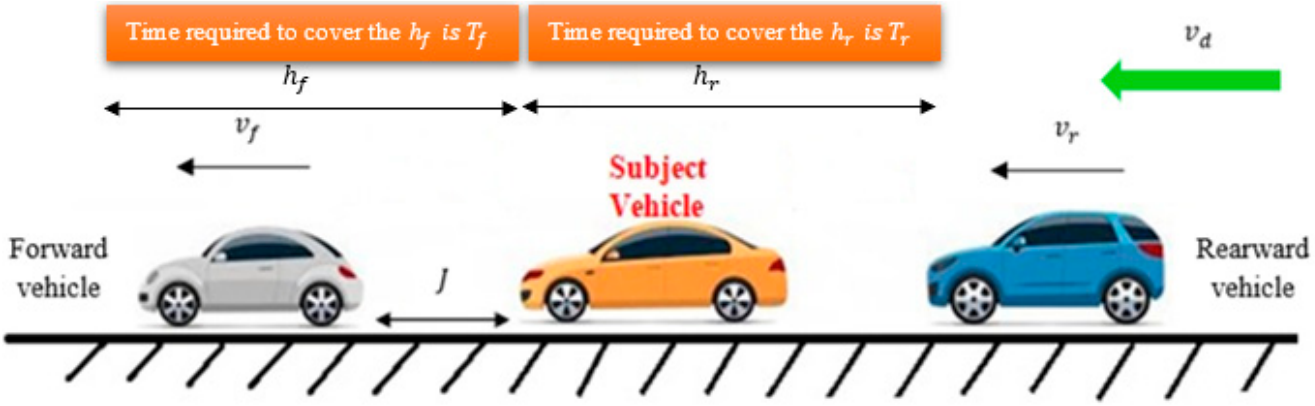

Figure 2. Proposed model parameters.

Driver sensitivity can be expressed as

$$\zeta = \frac{\tau}{\tau_s} \tag{7}$$

where τ_s is the safe time headway required to avoid accidents. When τ is less than τ_s, vehicles are slow and there is a small distance between them so drivers respond quickly. Conversely, when the time headway is greater than the safe time headway, the flow is smooth so the distance headway is large and driver response is slow. Substituting Equation (7) in Equation (6) gives the proposed acceleration exponent

$$\delta = \frac{\tau}{\tau_s}\left(\frac{h_f}{\tau_f} - \frac{h_r}{\tau_r}\right) \tag{8}$$

and replacing δ in Equation (1) with Equation (8), the proposed model is obtained as

$$\dot{v} = a_m\left(1 - \left(\frac{v}{v_d}\right)^{\frac{\tau}{\tau_s}\left(\frac{h_f}{\tau_f} - \frac{h_r}{\tau_r}\right)} - \left(\frac{s^*}{h}\right)^2\right), \tag{9}$$

This model employs the distance and time headways to account for vehicle alignment due to changes in traffic. This is more accurate than the ID model that relies on an arbitrary constant regardless of the traffic conditions. Further, this constant is not based on traffic physics.

Traffic density is the inverse of the distance headway and at steady state $\rho = 1/h_e$ where h_e is the equilibrium distance headway [40]. At steady state, $\Delta v = 0$ so substituting Equation (2) in Equation (1) and solving for h gives

$$h_e = (J + \tau v)\left(1 - \left(\frac{v}{v_d}\right)^{\delta}\right)^{-0.5} \tag{10}$$

for the ID model and

$$h_e = (J + \tau v)\left(1 - \left(\frac{v}{v_d}\right)^{\frac{T}{T_s}\left(\frac{h_f}{T_f} - \frac{h_r}{T_r}\right)}\right)^{-0.5} \tag{11}$$

for the proposed model. Equation (10) indicates that the ID model headway is based on an arbitrary fixed value δ and so is unrealistic. On the other hand, Equation (11) is based on actual traffic parameters such as the distance and time headways and so δ is not a constant.

The steady-state traffic flow is given by $F = \frac{v}{h_e}$ which for the ID model is

$$F = \frac{v}{(J + \tau v)\left(1 - \left(\frac{v}{v_d}\right)^{\delta}\right)^{-0.5}} \tag{12}$$

and for the proposed model is

$$F = \frac{v}{(J + \tau v)\left(1 - \left(\frac{v}{v_d}\right)^{\frac{T}{T_s}\left(\frac{h_f}{T_f} - \frac{h_r}{T_r}\right)}\right)^{-0.5}} \tag{13}$$

This indicates that the steady-state traffic flow for the proposed model incorporates the time and distance headways. With a small headway, driver response is quick as there are significant interactions between vehicles and drivers have little time to react. In this case, the traffic flow is low [9,41]. Conversely, with a large headway there are few vehicle interactions and driver response is slow. In addition, drivers have more time to react so the flow is high [9,41].

3. Performance Results

The proposed and ID models are evaluated using the Euler scheme [40] implemented in MATLAB. A circular road of length 2000 m is considered with periodic boundary conditions. The simulation time is 200 s and the time step is 0.5 s. The desired velocity is 30 m/s and the maximum and the minimum deceleration (negative deceleration) are 0.5 m/s^2 and 3 m/s^2, respectively [29]. The jam spacing is 2 m [37], and the forward and rearward distance headways are both 25 m [2]. The time headway varies depending on the traffic conditions and is usually between 0.5 s and 2.6 s [42]. Here, the forward time headway is 1.5 s, the rearward time headway is 1.6 s, and τ_s is 1.4 s. The ID model is evaluated for $\tau = 2$ s [6], while the proposed model is evaluated for $\tau = 0.6, 1, 1.5, 2$, and 2.2 s. The acceleration exponent varies from 1 to ∞ and is commonly set to 4 [22], so $\delta = 1, 4$ and 100 is considered. There are 52 vehicles on the road, each with a length of 4.5 m [43]. The simulation parameters are given in Table 1.

Table 1. Simulation Parameters.

Parameter	Value
Desired velocity, v_d	30 m/s
Time headway for ID model, τ	2 s
Forward and rearward distance headways, h_f and h_r	25 m
Forward time headway, τ_f	1.5 s
Rearward time headway, τ_r	1.6 s
Safe time headway, τ_s	1.4 s
Jam spacing, J	2 m
Maximum deceleration, a_m	0.5 m/s^2
Minimum deceleration, b	3 m/s^2
Time headway for the proposed model, τ	0.6, 1, 1.5, 2, and 2.2 s
Vehicle length, L	4.5 m
Acceleration exponent, δ	1, 4, and 100
Time step, Δt	0.5 s
Maximum normalized density, $\rho_m = 1/J$	0.5

Figure 3 presents the ID model velocity on a 2000 m circular road for $\delta = 1, 4$, and 100. When $\delta = 1$, the initial velocity is 6.7 m/s and increases to 22.5 m/s at 97 s. It then decreases to 0.86 m/s at 127 s and then increases to 8.5 m/s at 200 s. When $\delta = 4$, the velocity is 3.1 m/s at 138.5 s, increases to 15.9 m/s at 200 s, and then decreases to 0.07 m/s at 107.5 s. The highest velocity is 27.1 m/s at 78 s. When $\delta = 100$, the velocity increases

from 0.74 m/s at 1.5 s to 29.8 m/s from 62 s to 73.5 s. It decreases to 0.12 m/s at 101.5 s, increases to 1.5 m/s at 127 s, and is 16.7 m/s at 200 s.

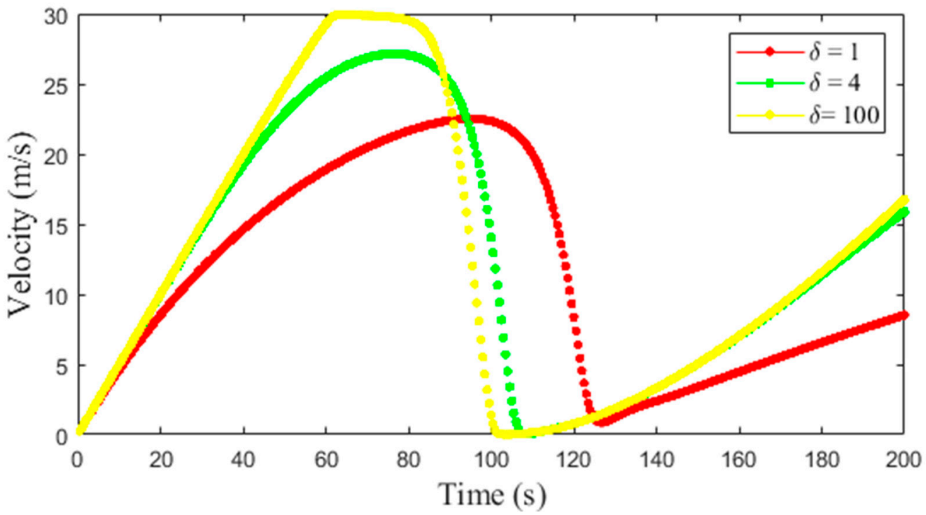

Figure 3. Velocity with the ID model for $\delta = 1, 4$, and 100 on a 2000 m circular road.

The velocity on a 2000 m circular road with the proposed model for $\tau = 0.6$, 1, 1.5, 2, and 2.2 s is shown in Figure 4. When $\tau = 0.6$ s, the initial velocity is 8.1 m/s and increases to 19.5 m/s at 127.5 s. It decreases to 11.0 m/s at 163 s and then increases to 15.0 m/s at 200 s. When $\tau = 1$ s, the initial velocity is 9.74 m/s and increases to 21.5 m/s at 108 s. It is 9.5 m/s at 142 s and 15.0 m/s at 200 s. When $\tau = 1.5$ s, the velocity increases from 10.7 m/s at 95 s to 23.0 m/s at 25.5 s. It decreases to 3.8 m/s at 125.5 s and then increases to 13.2 m/s at 200 s. When $\tau = 2$ s, the initial velocity is 10.1 m/s and increases to 24.1 m/s at 87.5 s. It decreases to 0.44 m/s at 119 s and then increases to 11.1 m/s at 200 s. When $\tau = 2.2$ s, the initial velocity is 10.4 m/s and increases to 24.3 m/s at 86 s. It is 0.12 m/s at 86 s and increases to 9.9 m/s at 200 s.

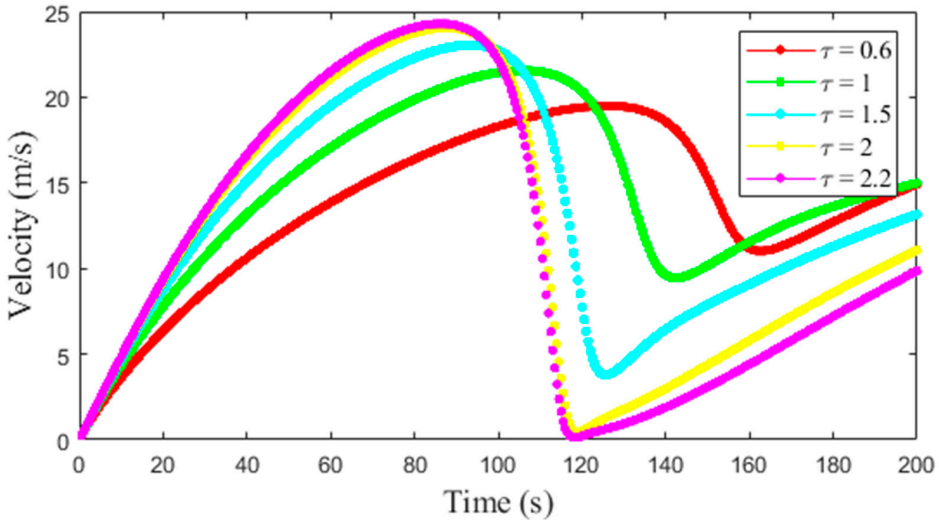

Figure 4. Velocity with the proposed model for $\tau = 0.6$, 1, 1.5, 2, and 2.2 s on a 2000 m circular road.

Figure 5 presents the flow with the ID model on a 2000 m circular road for $\delta = 1, 4$, and 100. When $\delta = 1$, the initial flow is 0.04 veh/s and increases to 0.54 veh/s at 122.5 s. It is 0.21 veh/s at 128 s and increases to 0.34 veh/s at 199.5 s. When $\delta = 4$, the initial flow is 0.05 veh/s and increases to 0.56 veh/s at 104.5 s. It decreases to 0.01 veh/s at 108.5 s and then increases to 0.31 veh/s at 140 s and 0.37 veh/s at 200 s. When $\delta = 100$, the initial flow is 0.04 veh/s, increases to 0.57 veh/s at 99 s, and then decreases to 0.002 veh/s at 104 s.

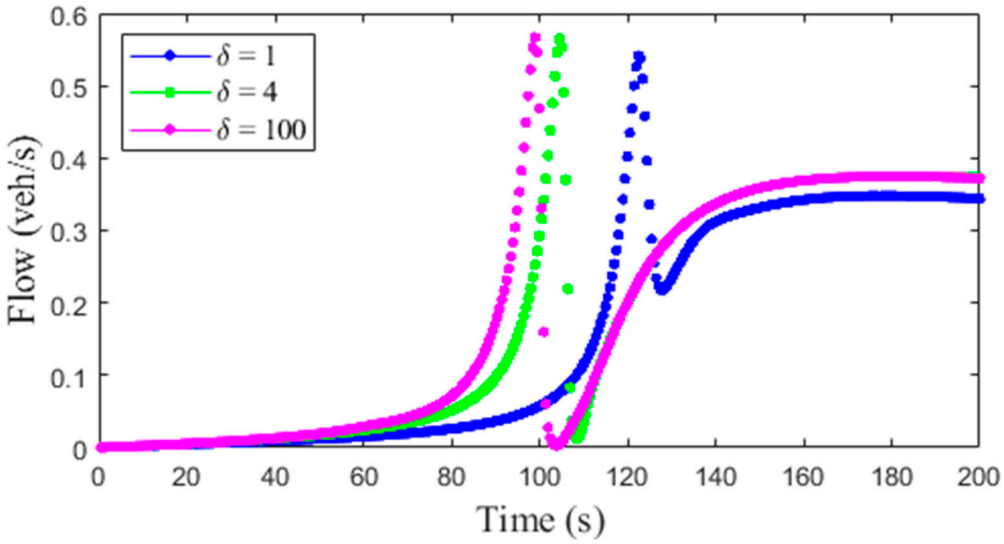

Figure 5. ID model flow for $\delta = 1, 4$, and 100 on a circular road of length 2000 m.

The flow on a 2000 m circular road with the proposed model for $\tau = 0.6, 1, 1.5, 2$, and 2.2 s is given in Figure 6. When $\tau = 0.6$ s, the flow is 0.07 veh/s at 130.5 s, increases to 0.83 veh/s at 161.5 s, and then decreases to 0.44 veh/s at 199.5 s. When $\tau = 1$ s, the flow is 0.05 veh/s at 106 s, increases to 0.72 veh/s at 140 s, and then decreases to 0.49 veh/s at 200 s. When $\tau = 1.5$ s, the flow is 0.06 veh/s at 99 s and increases to 0.66 veh/s at 122.5 s. It decreases to 0.39 veh/s at 134.5 s and then increases to 0.42 veh/s at 200 s. When $\tau = 2$ s, the flow is 0.07 veh/s at 98 s and then increases to 0.54 veh/s at 115.5 s. It decreases to 0.15 veh/s at 120 s and then increases to 0.36 veh/s at 200 s. When $\tau = 2.2$ s, the flow is 0.04 veh/s at 90.5 s and increases to 0.51 veh/s at 114 s. It is 0.05 veh/s at 119 s and increases to 0.33 veh/s at 200 s.

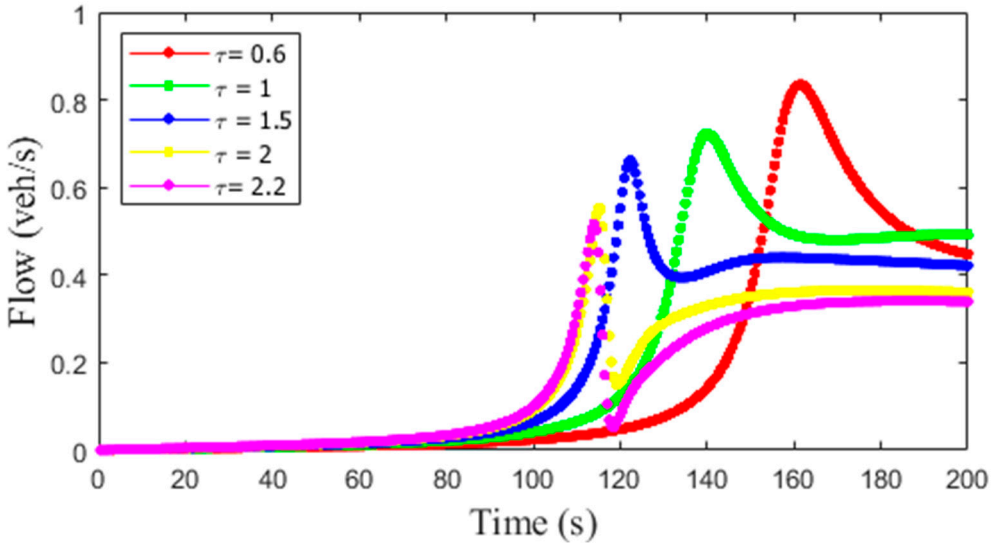

Figure 6. Proposed model flow for $\tau = 0.6, 1, 1.5, 2$, and 2.2 s on a circular road of length 2000 m.

Figure 7 presents the trajectories of a platoon of 52 vehicles with the ID model on a 2000 m circular road, and the results at 90 s are given in Table 2. The thick black line is the trajectory of the 1st vehicle while the pink lines show the trajectories of the following 51 vehicles. When $\delta = 1$, Figure 7a shows that the position of the 1st and 15th vehicles is 1286 m and 266.9 m, respectively, while the position of the 30th and 50th vehicles is -23.1 m and -96.0 m, respectively. When $\delta = 4$, Figure 7b shows that the position of the 1st and 15th vehicles is 1640 m and 383.1 m, respectively, while the position of the 30th and

50th vehicles is −14.0 m and −96.0 m, respectively. When $\delta = 100$, Figure 7c shows that the position of the 1st and 15th vehicles is 1762 m and 396.0 m, respectively, while the position of the 30th and 50th vehicles is −2.3 m and −96.0 m, respectively.

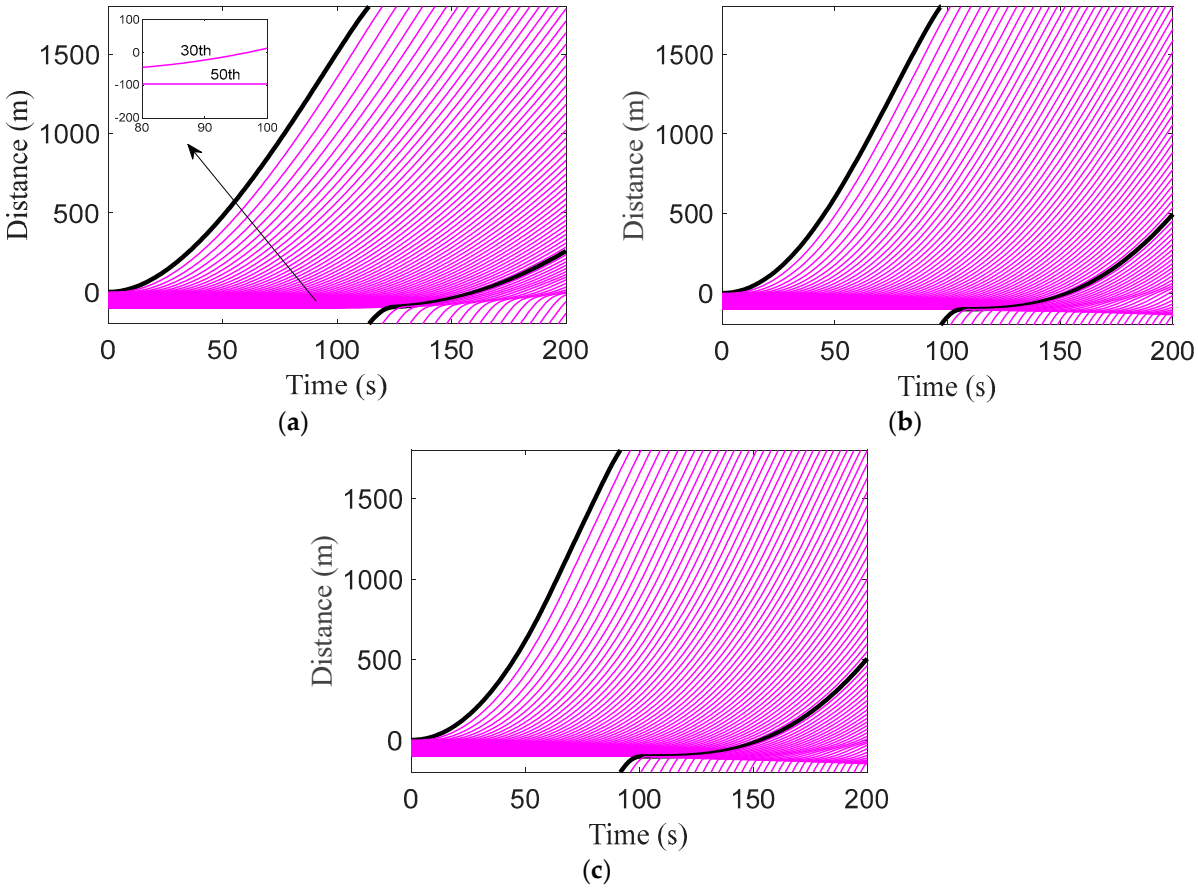

Figure 7. ID model trajectories on a 2000 m circular road for (**a**) $\delta = 1$, (**b**) $\delta = 4$, and (**c**) $\delta = 100$.

Table 2. Position of the 1st, 15th, 30th, and 50th vehicles at 90 with the ID model on a 2000 m circular road.

Acceleration Exponent δ	1st Vehicle Position (m)	15th Vehicle Position (m)	30th Vehicle Position (m)	50th Vehicle Position (m)
1	1286	266.9	−23.1	−96.0
4	1639	383.1	−14.0	−96.0
100	1762	396.0	−2.3	−96.0

The trajectories of a platoon of 52 vehicles with the proposed model on a 2000 m circular road are presented in Figure 8, and the results at 90 s are given in Table 3. The first vehicle is denoted by a thick pink line, while the following 51 vehicles are shown by black lines. When $\tau = 0.6$ s, Figure 8a shows that the 1st vehicle position is 956.5 m and the 15th vehicle position is 395.0 m, whereas the 30th and 50th vehicle positions are 69.8 m and −96.0 m, respectively. When $\tau = 1$ s, Figure 8b shows that the 1st vehicle position is 1171 m and the 15th vehicle position is 422.8 m, whereas the 30th and 50th vehicle positions are 78.1 m and −95.9 m, respectively. When $\tau = 1.5$ s, Figure 8c shows that the 1st vehicle position is 1325 m and the 15th vehicle position is 426.4 m, whereas the 30th and 50th vehicle positions are 47.0 m and −96.0 m, respectively. When $\tau = 2$ s, Figure 8d shows that the 1st vehicle position is 1432 m and the 15th vehicle position is 327.8 m, whereas the 30th and 50th vehicle positions are −5.7 m and −96.0 m, respectively. When $\tau = 2.2$ s,

Figure 8e shows that the 1st vehicle position is 1443 m and the 15th vehicle position is 338.3 m, whereas the 30th and 50th vehicle positions are −20.9 m and −96.0 m, respectively.

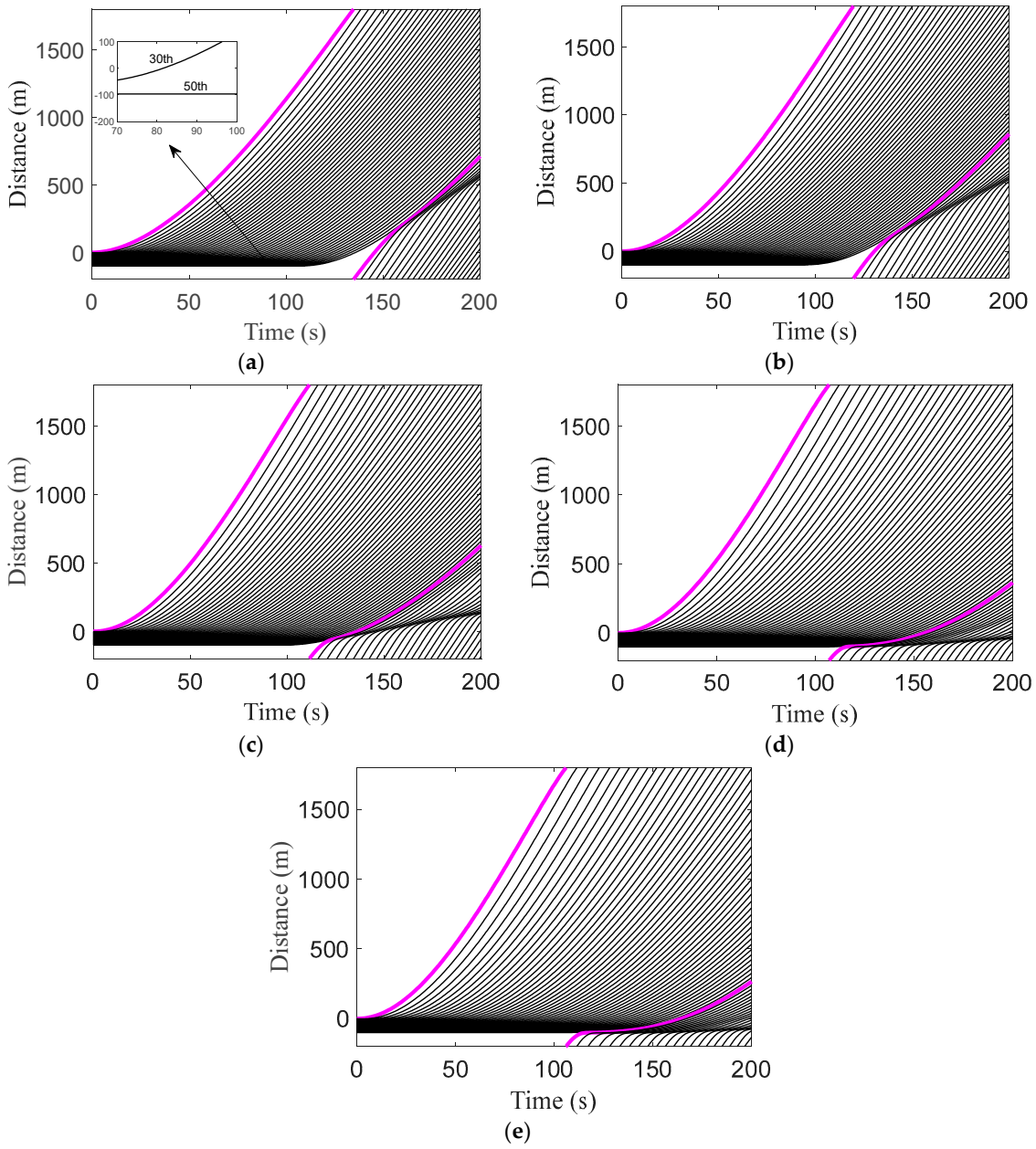

Figure 8. Proposed model trajectories on a 2000 m circular road for (**a**) $\tau = 0.6$ s, (**b**) $\tau = 1$ s, (**c**) $\tau = 1.5$, (**d**) $\tau = 2$ s, and (**e**) $\tau = 2.2$ s.

Table 3. Position of the 1st, 15th, 30th, and 50th vehicles at 90 s with the proposed model on a 2000 m circular road.

Time Headway τ (s)	1st Vehicle Position (m)	15th Vehicle Position (m)	30th Vehicle Position (m)	50th Vehicle Position (m)
0.6	956.5	395.0	69.8	−96.0
1	1171	422.8	78.1	−95.9
1.5	1325	426.4	47.0	−96.0
2	1432	327.8	−5.7	−96.0
2.2	1443	338.3	−20.9	−96.0

Figure 9 presents the density with the ID model over time and space on a 2000 m circular road and Table 4 gives the congestion results. When $\delta = 1$, Figure 9a shows that there is congestion from 0 s to 101 s as the density is 0.50. At −93.0 m, it decreases to 0.29 at 125.5 s and 0.15 at 198.5 s. At 199 s, the density is 0.15 at −9.0 m and decreases to 0.012 at 1791 m. When $\delta = 4$, Figure 9b shows that there is congestion from 0 s to 103 s as the density is 0.50. It is between 0.26 and 0.50 from 110.5 s to 200 s. At 198 s, the density is 0.50 at −132.0 m and decreases to 0.10 at −54.0 m and 0.02 at 1785 m. When $\delta = 100$, Figure 9c shows that there is congestion between −99.0 m and −3.0 m as the density is 0.50, and at −144.0 m this continues until 200 s. At 198 s, the density is 0.5 at −144.0 and decreases to 0.07 at −21.0 m and 0.01 at 1791 m.

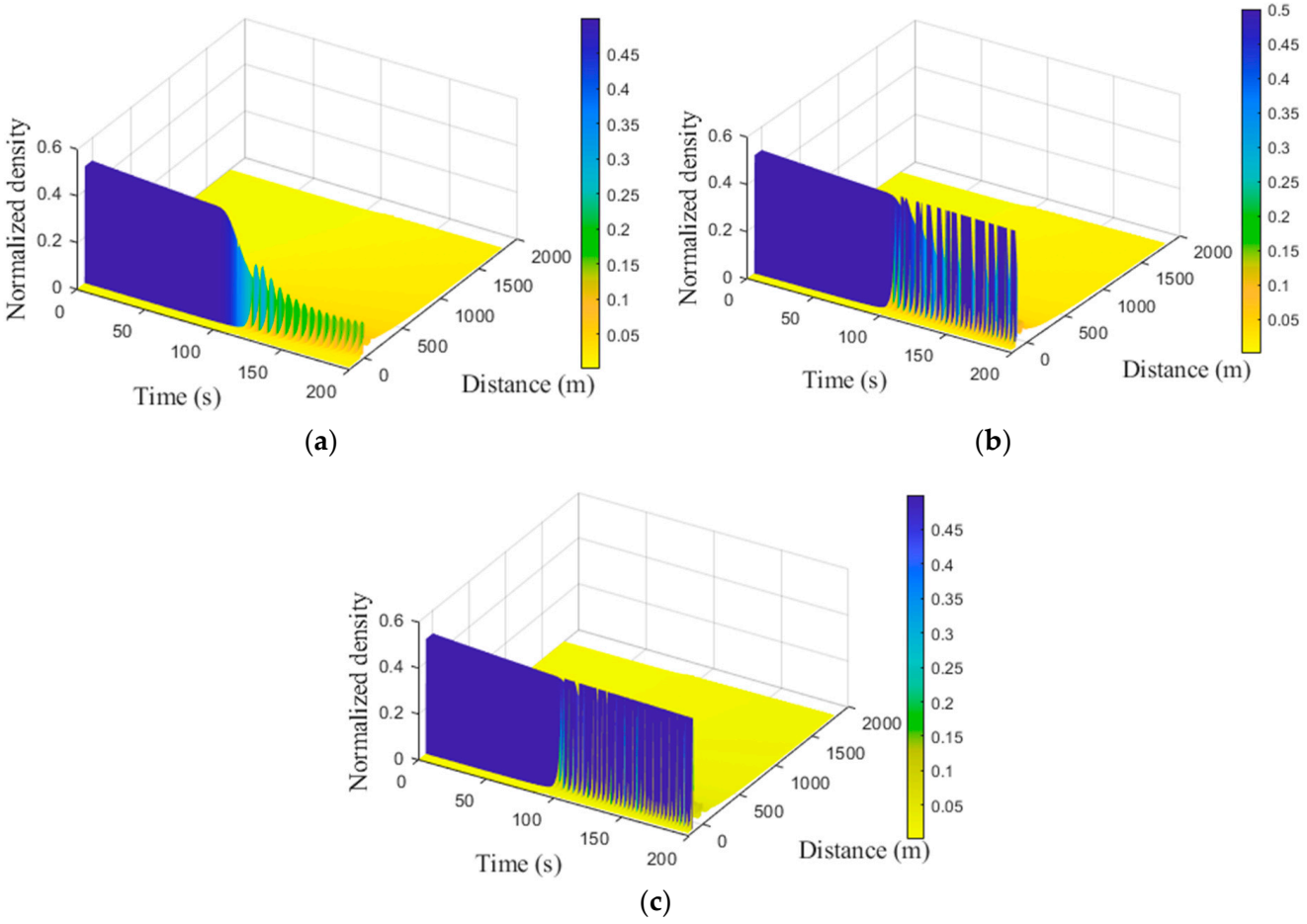

Figure 9. ID model density on a 2000 m circular road for (**a**) $\delta = 1$, (**b**) $\delta = 4$, and (**c**) $\delta = 100$.

Table 4. ID model density and time during and after congestion.

Acceleration Exponent δ	Time during Which Congestion Occurs (s)	Density during Congestion	Density after Congestion Dissipates	Time after Congestion Dissipates (s)
1	0–101	0.50	0.29	125.5
4	0–103	0.50	0.26–0.50	110.5–200
100	0–200	0.50	Congestion does not dissipate	-

The density with the proposed model over time and space on a 2000 m circular road is given in Figure 10 and Table 5 gives the congestion results. When $\tau = 0.6$ s, Figure 10a shows that there is congestion from 0 s to 102 s as the density is 0.50. It decreases to 0.01 at

78.0 m and 146 s and then increases to 0.09 at 564.0 m and 200 s. At 199 s, the density is 0.02 between 0 m and 477.0 m and decreases to 0.02 at 1722 m. When $\tau = 1$ s, Figure 10b shows that the density is 0.50 from 0 s to 89.5 s which indicates congestion. After the congestion dissipates, the density is 0.02 at 129 s and 33.0 m, and increases to 0.09 at 199.5 s and 525.0 m. Between 0 m and 462 m, the density is 0.02 at 198 s. It increases to 0.09 at 525.0 m and then decreases to 0.02 at 1779 m. When $\tau = 1.5$ s, Figure 10c shows there is congestion from 0 s to 93 s as the density is 0.50. The density decreases to 0.15 at -54.0 m and 124 s and then increases to 0.18 at 129.0 m and 199.5 s. At 200 s, the density between 0 m and 66.0 m is 0.15 and decreases to 0.02 at 1773 m. When $\tau = 2$ s, Figure 10d shows there is congestion between 0 s and 96 s as the density is 0.50. At -96.0 m, it decreases to 0.36 at 118.5 s and 0.20 at 198 s. At 198.5 s, the density is 0.20 at -42.0 m and decreases to 0.06 at 99.0 m and 0.01 at 1746 m. When $\tau = 2.2$ s, Figure 10e shows there is congestion between 0 s and 103 s as the density of 0.5. It decreases to 0.45 at -99.0 m and 117 s and 0.19 at -75.0 m and 199 s. At 199 s, the density is 0.07 at 18.0 m and 0.01 at 1767 m.

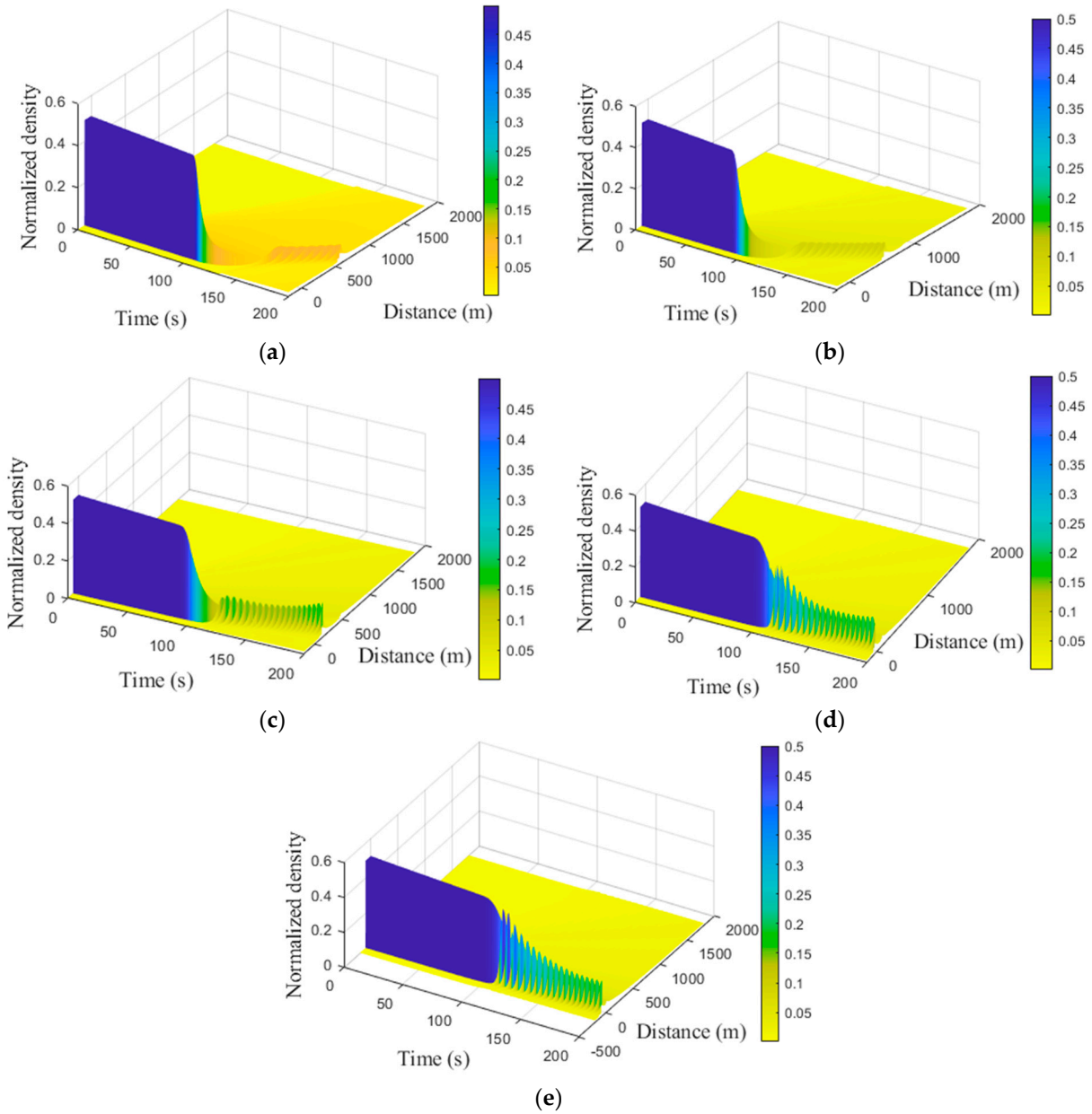

Figure 10. Proposed model density on a 2000 m circular road for (**a**) $\tau = 0.6$ s, (**b**) $\tau = 1$ s, (**c**) $\tau = 1.5$ s, (**d**) $\tau = 2$ s, and (**e**) $\tau = 2.2$ s.

Table 5. Proposed model density and time during and after congestion.

Time Headway τ (s)	Time during Which Congestion Occurs (s)	Density during Congestion	Density after Congestion Dissipates	Time after Congestion Dissipates (s)
0.6	0–102	0.50	0.01	146
1	0–89.5	0.50	0.02	129
1.5	0–93	0.50	0.15	124
2	0–96	0.50	0.36	118.5
2.2	0–103	0.50	0.45	117

Figure 11 presents the ID model flow for $\delta = 1, 4$, and 100. When $\delta = 1$, Figure 11a shows that at -204.0 m the flow is zero from 0 s to 100 s. It is 0.54 veh/s at 123 s and 0.55 veh/s at 196.5 s. At -12.0 m, the flow is 0.52 veh/s at 199.5 s, and decreases to 0.37 veh/s at 93.0 m and 0.25 veh/s at 1743 m. When $\delta = 4$, Figure 11b shows that at -180.0 m the flow is zero from 0 s to 90 s. It increases to 2.13 veh/s at 112.5 s and varies between 0.67 veh/s and 6.05 veh/s from 131.5 s to 198.5 s. At 196 s, the flow is 0.24 veh/s at -96.0 m and increases to 0.38 veh/s at 144.0 m where it remains. When $\delta = 100$, Figure 11c shows that at -141.0 m, the flow is zero from 0 s to 84 s. It increases to 4.11 veh/s at 106.5 s and varies between 9.17 veh/s and 3.20 veh/s from 124.5 s to 200 s. At 200 s, the flow is 0.24 veh/s at -114.0 m and increases to 0.37 veh/s at 174.0 m where it remains.

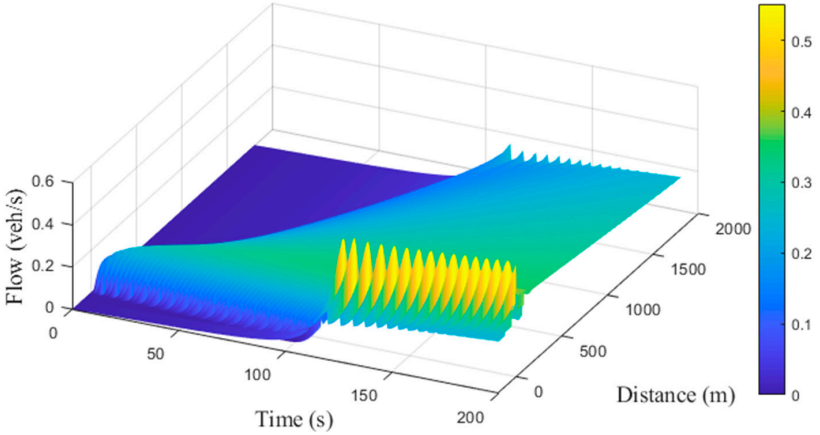

(**a**)

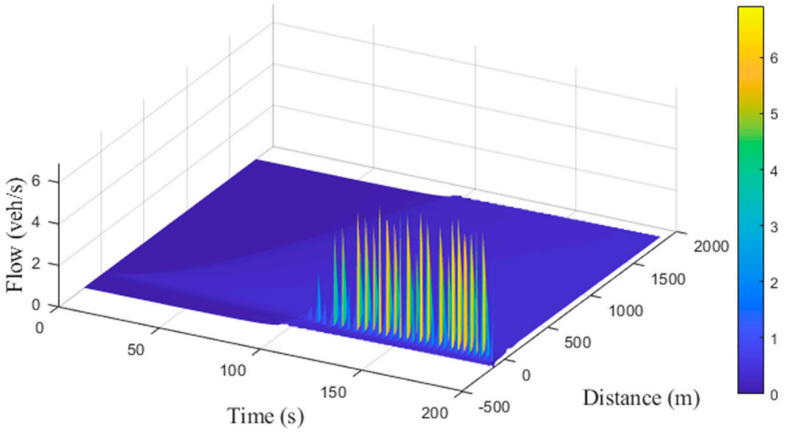

(**b**)

Figure 11. *Cont.*

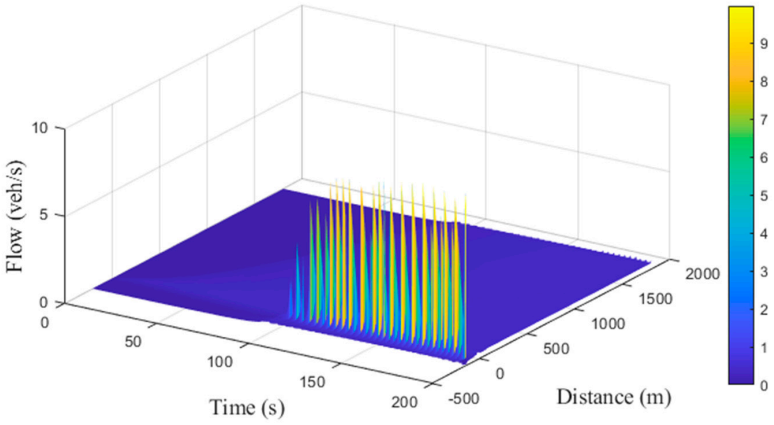

(**c**)

Figure 11. Flow with the ID model on a 2000 m circular road for (**a**) $\delta = 1$, (**b**) $\delta = 4$, and (**c**) $\delta = 100$.

Figure 12 presents the flow with the proposed model on a 2000 m circular road for $\tau = 0.6$, 1, 1.5, 2, and 2.2 s. When $\tau = 0.6$ s, Figure 12a shows that at -174.0 m, the flow is zero from 0 s to 118 s. It increases to 1.04 veh/s at 225 s and then decreases to 1.00 veh/s at 199 s. At 198 s, the flow is 0.40 veh/s between 0 m and 276.0 m and increases to 1.01 veh/s at 540.0 m. It then decreases to 0.43 veh/s at 753.0 m and remains constant. When $\tau = 1$ s, Figure 12b shows that at -201.0 m, the flow is zero from 0 s to 111 s. It increases to 0.82 veh/s at 142.5 s and is approximately constant until 200 s. At 198 s, the flow is 0.36 veh/s between 0 m and 102.0 m and increases to 0.84 veh/s at 510.0 m. It decreases to 0.49 veh/s at 864.0 m and 0.40 veh/s at 1734 m. When $\tau = 1.5$ s, Figure 12c shows that at -159.0 m the flow is zero from 0 s to 91 s. It increases to 0.69 veh/s at 125.5 s and is approximately constant until 200 s. At 199 s, the flow is 0.32 veh/s between 0 m and 63.0 m and increases to 0.69 veh/s at 129.0 m. It decreases to 0.48 veh/s at 450.0 m and 0.33 veh/s at 1767 m. When $\tau = 2$, Figure 12d shows that at -201.0 m, the flow is zero from 0 s to 84 s. It increases to 0.54 veh/s at 115.5 s and is approximately constant until 200 s. At 199 s, the flow is 0.56 veh/s at -48.0 m and decreases to 0.41 veh/s at 96.0 m and 0.28 veh/s at 1785 m. When $\tau = 2.2$ s, Figure 12e shows that at -171.0 m, the flow is zero from 0 s to 83 s. It increases to 0.50 veh/s at 113.5 s and 0.52 veh/s at 197 s. At 199.5 s, the flow is 0.52 veh/s at -81.0 m and decreases to 0.35 veh/s at 24.0 m and 0.27 veh/s at 1773 m.

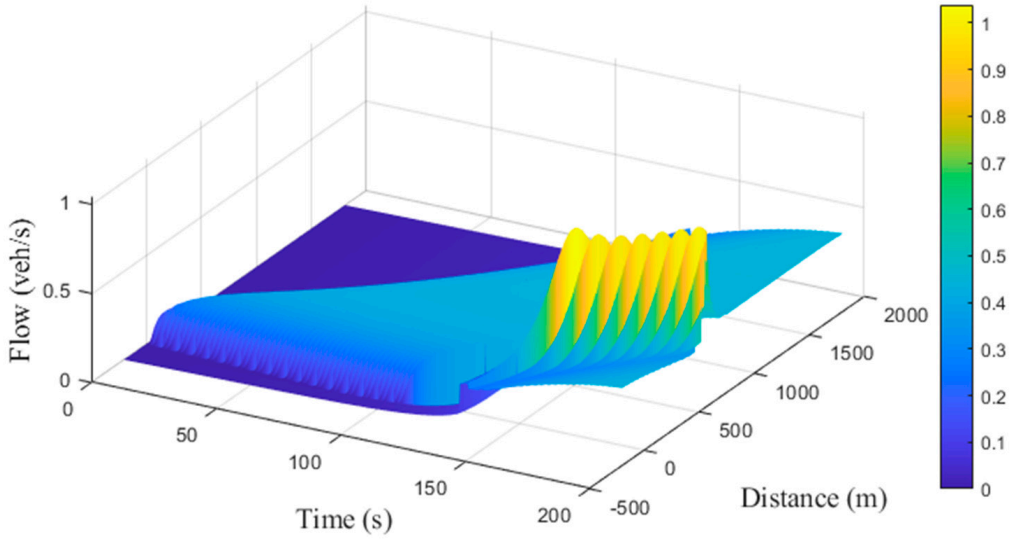

(**a**)

Figure 12. *Cont.*

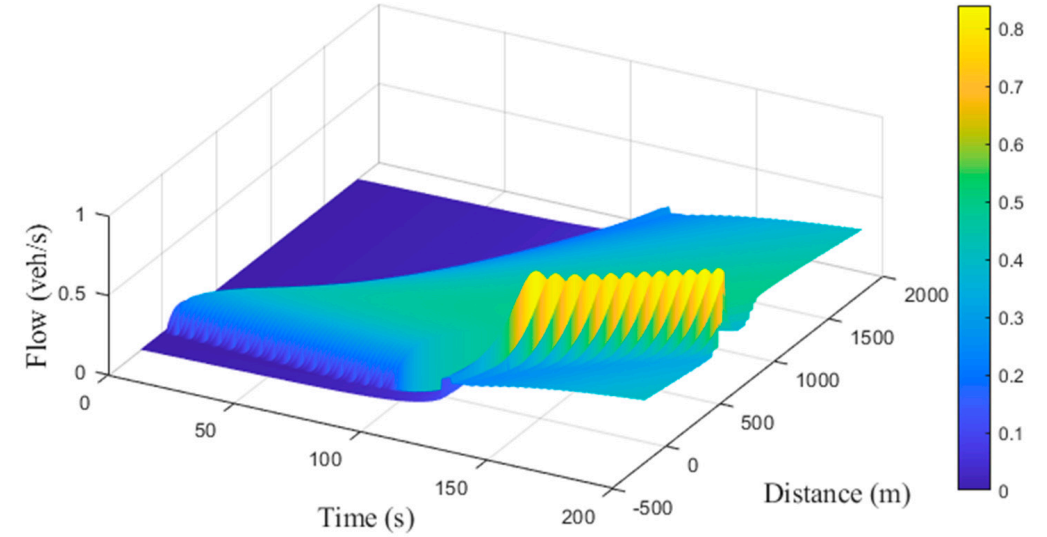

(**b**)

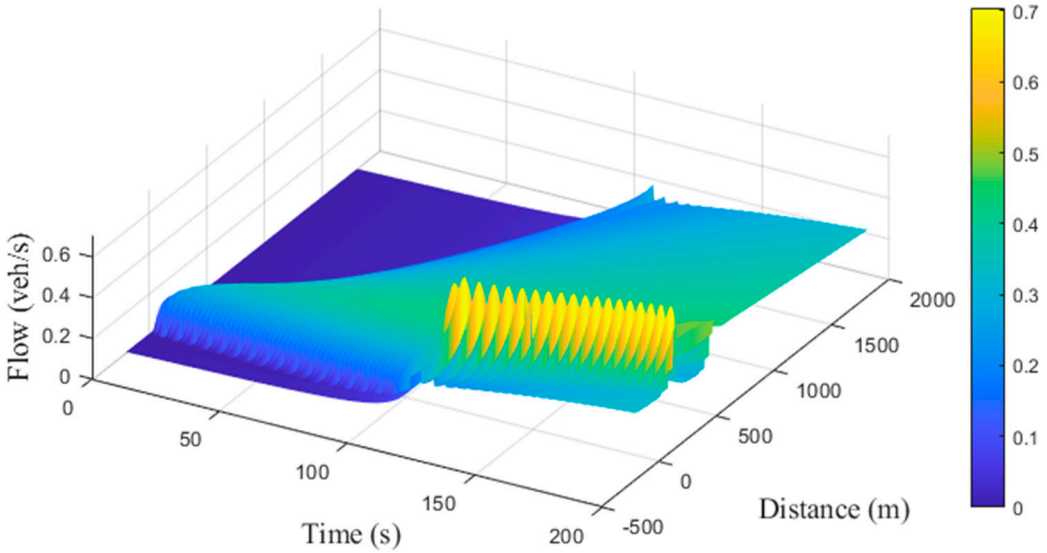

(**c**)

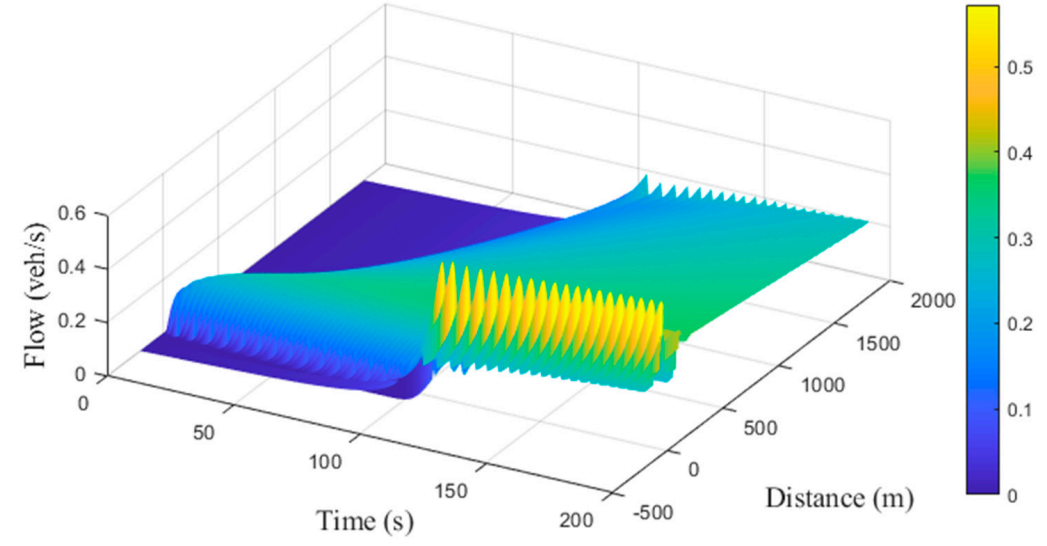

(**d**)

Figure 12. *Cont.*

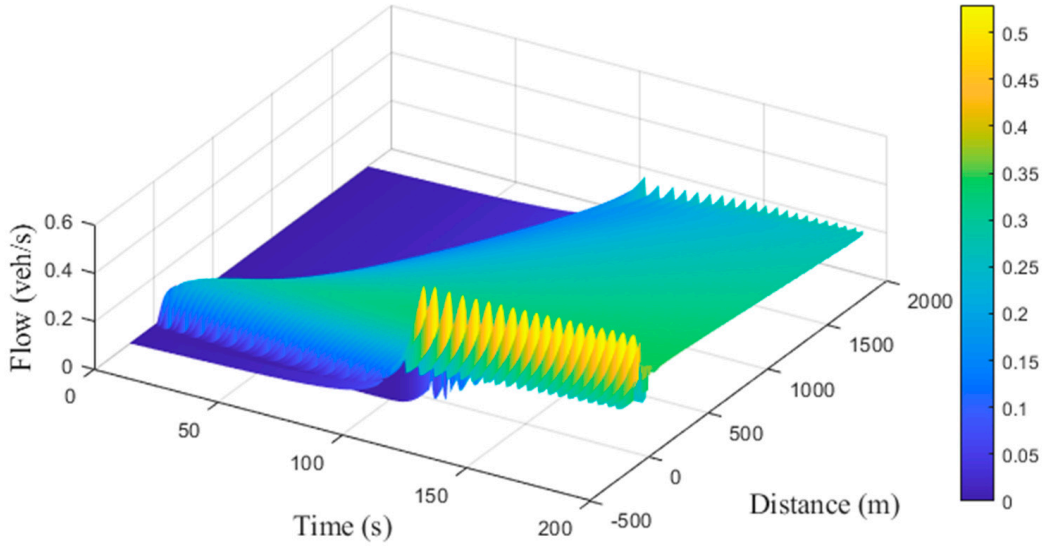

(**e**)

Figure 12. Flow with the proposed model on a 2000 m circular road for (**a**) $\tau = 0.6$ s, (**b**) $\tau = 1$ s, (**c**) $\tau = 1.5$ s, (**d**) $\tau = 2$ s, and (**e**) $\tau = 2.2$ s.

4. Discussion

The results presented in Figure 3 indicate that the variations in velocity with the ID model increase with the acceleration exponent δ. Further, Figure 4 illustrates that the variations in velocity with the proposed model increase with the time headway. Figure 5 shows that the variations in flow with the ID model increase over time as δ increases. Similarly, the results for the proposed model presented in Figure 6 indicate that the variations in flow over time increase with a larger time headway.

Figures 7 and 8 present the vehicle trajectories in time and space with the ID and proposed models, respectively, and the results are summarized in Tables 2 and 3. Table 2 indicates that as δ increases, the distance traveled by the 1st and 15th vehicles increases, while that traveled by the 30th vehicle decreases. However, the distance traveled by the 50th vehicle is approximately the same. Table 3 shows that a decrease in the time headway decreases the distance traveled by the 1st vehicle, while the distance traveled by the 15th vehicle increases between 0.6 s and 1.5 s, decreases between 1.5 s and 2.0 s, and then increases. Between 0.6 s and 1.0 s, the distance traveled by the 30th vehicle increases and then decreases between 1.0 s and 2.2 s. The distance traveled by the 50th vehicle decreases between 0.6 s and 1.0 s and then increases. These results show that the vehicle positions with the ID model obtained using an arbitrary constant are not based on real traffic conditions. Conversely, the positions according to the proposed model are based on the time headway. This results in a smooth flow with the platoon of vehicles which is more realistic than the ID model.

Figure 9 shows that as δ increases, the ID model density increases over time so there is congestion with a large δ. Moreover, Figure 11 indicates that the flow increases with δ. Figure 10 shows that the density with the proposed model is small for a small time headway and vice versa. In addition, Figure 12 indicates that the changes in flow are proportional to the time headway.

Overall, the results given indicate that the traffic behavior with the proposed model is more realistic than with the ID model. In particular, the flow and velocity are smoother, and the variations in flow and density over time are smaller. The ID model can produce unrealistic traffic behavior such as the significant congestion shown in Figure 9c. This is because the ID model employs an arbitrary constant whereas in the proposed model this constant is replaced with a variable based on the time headway. The results presented

highlight the importance of considering real traffic parameters in traffic flow models to accurately characterize traffic behavior.

5. Conclusions

A microscopic traffic model was proposed which improves the well know ID model. The proposed model considers the velocity differences between forward and rearward vehicles. It was evaluated on a 2000 m circular road for different values of time headway. The results obtained demonstrate that the traffic density and flow with the proposed model are realistic. In contrast, the ID model provides poor results due to inappropriate traffic characterization. In particular, constant vehicle speeds are considered which do not reflect real driving behavior. The proposed model incorporates time headway to provide a more accurate characterization of vehicle movement. As a result, the variations in flow and velocity are smoother than with the ID model.

The proposed microscopic model can be employed in ACC and cooperative ACC systems, as well as in automated vehicles, to make traffic safe and efficient. In addition, it can be incorporated into traffic simulators to provide realistic traffic predictions. Future research can consider heterogeneous traffic based on real-time data acquired from roadside units.

Author Contributions: Conceptualization, Z.H.K. and F.A.; methodology, Z.H.K. and F.A.; software, F.A.; validation, Z.H.K., F.A., A.B.A. and K.S.K.; formal analysis, F.A., Z.H.K., A.B.A. and K.S.K.; investigation, Z.H.K., F.A., A.B.A. and K.S.K.; writing—original draft, F.A.; writing—review and editing, Z.H.K., F.A. and T.A.G.; visualization, Z.H.K., F.A., A.B.A., T.A.G. and K.S.K.; funding acquisition, Z.H.K., A.B.A., T.A.G. and K.S.K. All authors have read and agreed to the published version of the manuscript.

Funding: This research received no external funding.

Institutional Review Board Statement: Not applicable.

Informed Consent Statement: Not applicable.

Data Availability Statement: Not applicable.

Conflicts of Interest: The authors declare no conflict of interest.

References

1. Azlan, N.N.N.; Rohani, M.M. Overview of application of traffic simulation model. In *MATEC Web of Conferences*; EDP Sciences: Johor, Malaysia, 2018.
2. Khan, Z.H.; Gulliver, T.A. A macroscopic traffic model based on anticipation. *Arab. J. Sci. Eng.* **2019**, *44*, 5151–5163. [CrossRef]
3. Khan, Z.H.; Gulliver, T.A.; Azam, K.; Khattak, K.S. A macroscopic model based on driver physiological and psychological behavior due to changes in traffic. *J. Eng. Appl. Sci.* **2019**, *38*, 1–9.
4. Toledo, T.; Koutsopoulos, H.N.; Ben-Akiva, M. Integrated driving behavior modeling. *Transp. Res. Part C Emerg. Technol.* **2007**, *15*, 96–112. [CrossRef]
5. Zhang, L.; Zhang, S.; Zhou, B.; Jiao, S.; Huang, Y. An improved car-following model considering desired safety distance and heterogeneity of driver's sensitivity. *J. Adv. Transp.* **2021**, *2021*, 6693433. [CrossRef]
6. Ali, F.; Khan, Z.H.; Khattak, K.S.; Gulliver, T.A.; Khan, A.N. A microscopic heterogeneous traffic flow model considering distance headway. *Mathematics* **2021**, *11*, 184. [CrossRef]
7. Traffic Congestion Costs, U.S. Cities Billions of Dollars Every Year [Infographic]. Available online: https://www.forbes.com/sites/niallmccarthy/2020/03/10/traffic-congestion-costs-us-cities-billions-of-dollars-every-year-infographic/?sh=528a08c44ff8 (accessed on 1 January 2023).
8. The Number of Cars in the US in 2022/2023: Market Share, Distribution, and Trends—Financesonline.com. Available online: https://financesonline.com/number-of-cars-in-the-us/ (accessed on 29 December 2022).
9. Ali, F.; Khan, Z.H.; Khan, F.A.; Khattak, K.S.; Gulliver, T.A. A new driver model based on driver response. *Appl. Sci.* **2022**, *12*, 5390. [CrossRef]
10. Khan, Z. Traffic Modelling for Intelligent Transportation Systems. Ph.D. Dissertation, University of Victoria, Victoria, BC, Canada, 2016.

11. Ali, F.; Khan, Z.H.; Khattak, K.S.; Gulliver, T.A. A microscopic traffic flow model characterization for weather conditions. *Appl. Sci.* **2022**, *12*, 12981. [CrossRef]
12. Henein, C.M.; White, T. Microscopic information processing and communication in crowd dynamics. *Phys. A Stat. Mech. Its Appl.* **2010**, *389*, 4636–4653. [CrossRef]
13. Hoogendoorn, S.P.; Bovy, P.H.L. State-of-the-art of vehicular traffic flow modelling. *Proc. Inst. Mech. Eng. Part I J. Syst. Control Eng.* **2001**, *215*, 283–303. [CrossRef]
14. Pipes, L.A. An operational analysis of traffic dynamics. *J. Appl. Phys.* **1953**, *24*, 274–281. [CrossRef]
15. Reuschel, A. Vehicle movements in a platoon. *Oesterreichisches Ing. Archir.* **1950**, *4*, 193–215.
16. Askari, A.; Farias, D.A.; Kurzhanskiy, A.A.; Varaiya, P. Measuring impact of adaptive and cooperative adaptive cruise control on throughput of signalized intersections. *arXiv* **2016**, arXiv:1611.08973.
17. Newell, G.F. Nonlinear effects in the dynamics of car following. *Oper. Res.* **1961**, *9*, 209–229. [CrossRef]
18. Bando, M.; Hasebe, K.; Nakayama, A.; Shibata, A.; Sugiyama, Y. Dynamical model of traffic congestion and numerical simulation. *Phys. Rev. E* **1995**, *51*, 1035–1042. [CrossRef] [PubMed]
19. Helbing, D.; Tilch, B. Generalized force model of traffic dynamics. *Phys. Rev. E* **1998**, *58*, 133–138. [CrossRef]
20. Jiang, R.; Wu, Q.; Zhu, Z. Full velocity difference model for a car-following theory. *Phys. Rev. E* **2001**, *64*, 17101. [CrossRef] [PubMed]
21. Gipps, P.G. A behavioural car-following model for computer simulation. *Transp. Res. Part B* **1981**, *15*, 105–111. [CrossRef]
22. Treiber, M.; Hennecke, A.; Helbing, D. Congested traffic states in empirical observations and microscopic simulations. *Phys. Rev. E* **2000**, *62*, 1805–1824. [CrossRef]
23. Cao, Z.; Lu, L.; Chen, C.; Chen, X.U. Modeling and simulating urban traffic flow mixed with regular and connected vehicles. *IEEE Access* **2021**, *9*, 10392–10399. [CrossRef]
24. Kesting, A.; Treiber, M.; Helbing, D. Enhanced intelligent driver model to access the impact of driving strategies on traffic capacity. *Philos. Trans. R. Soc. A Math. Phys. Eng. Sci.* **2010**, *368*, 4585–4605. [CrossRef]
25. Derbel, O.; Peter, T.; Zebiri, H.; Mourllion, B.; Basset, M. Modified intelligent driver model for driver safety and traffic stability improvement. *IFAC Proc.* **2013**, *46*, 744–749. [CrossRef]
26. Dahui, W.; Ziqiang, W.; Ying, F. Hysteresis phenomena of the intelligent driver model for traffic flow. *Phys. Rev. E* **2007**, *76*, 2–8. [CrossRef] [PubMed]
27. Yang, S. Enlarged Stopping Distance to Improve Vehicle Discharge at Urban Signalised Intersections. Ph.D. Thesis, Queensland University of Technology, Brisbane, QLD, Australia, 2013.
28. Kovács, T.; Bolla, K.; Gil, R.A.; Fábián, C.; Kovács, L. Parameters of the intelligent driver model in signalized intersections. *Teh. Vjesn.* **2016**, *23*, 1469–1474.
29. Liebner, M.; Baumann, M.; Klanner, F.; Stiller, C. Driver intent inference at urban intersections using the intelligent driver model. In Proceedings of the IEEE Intelligent Vehicle Symposium, Madrid, Spain, 3–7 June 2012.
30. Salles, D.; Kaufmann, S.; Reuss, H.-C. Extending the intelligent driver model in SUMO and verifying the drive off trajectories with aerial measurements. In Proceedings of the SUMO Conference, Virtual, 26–28 October 2020.
31. Liu, P.; Fan, W. Exploring the impact of connected and autonomous vehicles on freeway capacity using a revised intelligent driver model. *Transp. Plan. Technol.* **2020**, *43*, 279–292. [CrossRef]
32. Rahman, M.; Islam, M.R.; Chowdhury, M.; Khan, T. Development of a connected and automated vehicle longitudinal control model. *arXiv* **2020**, arXiv:2001.00135.
33. Li, Y.; Li, Z.; Wang, H.; Wang, W.; Xing, L. Evaluating the safety impact of adaptive cruise control in traffic oscillations on freeways. *Accid. Anal. Prev.* **2017**, *104*, 137–145. [CrossRef]
34. Schakel, W.J.; Van Arem, B.; Netten, B.D. Effects of cooperative adaptive cruise control on traffic flow stability. In Proceedings of the International IEEE Conference on Intelligent Transportation Systems, Funchal, Portugal, 19–22 September 2010.
35. Milanés, V.; Shladover, S.E.; Spring, J.; Nowakowski, C.; Kawazoe, H.; Nakamura, M. Cooperative adaptive cruise control in real traffic situations. *IEEE Trans. Intell. Transp. Syst.* **2013**, *15*, 296–305. [CrossRef]
36. Jafaripournimchahi, A.; Cai, Y.; Wang, H.; Sun, L.; Weng, J. Integrated-hybrid framework for connected and autonomous vehicles microscopic traffic flow modelling. *J. Adv. Transp.* **2002**, *2022*, 2253697. [CrossRef]
37. Malinauskas, R. The Intelligent Driver Model: Analysis and Application to Adaptive Cruise Control. Ph.D. Thesis, Clemson University, Clemson, SC, USA, 2014.
38. Rahman, M.; Islam, M.R.; Chowdhury, M.; Khan, T. A physics-based longitudinal driver model for automated vehicles. *IEEE Access* **2022**, *10*, 80883–80899. [CrossRef]
39. Halim, H.; Adisasmita, S.A.; Ramli, M.I.; Aly, S.H. The relationship of volume and headway on heterogeneous traffic conditions in Makassar City. In Proceedings of the IOP Conference Series: Earth and Environmental Science, Bali, Indonesia, 29–30 August 2019.
40. Kessels, F. *Traffic Flow Modelling: Introduction to Traffic Flow Theory through a Genealogy of Models*; Springer: Cham, Switzerland, 2019.
41. Khan, Z.H.; Gulliver, T.A.; Khattak, K.S. A novel macroscopic traffic model based on distance headway. *Civ. Eng. J.* **2021**, *8197*, 32–40. [CrossRef]

42. Taieb-Maimon, M.; Shinar, D. Minimum and comfortable driving headways: Reality versus perception. *Hum. Factors* **2001**, *43*, 159–172. [CrossRef] [PubMed]
43. Smart Motorist. How Long Is a Car? (Average Car Length According to Types). Available online: https://www.smartmotorist.com/average-car-length (accessed on 3 January 2023).

Disclaimer/Publisher's Note: The statements, opinions and data contained in all publications are solely those of the individual author(s) and contributor(s) and not of MDPI and/or the editor(s). MDPI and/or the editor(s) disclaim responsibility for any injury to people or property resulting from any ideas, methods, instructions or products referred to in the content.